

Reentrant Phase Behavior in Active Colloids with Attraction

Gabriel S. Redner, Aparna Baskaran, and Michael F. Hagan*
Martin Fisher School of Physics, Brandeis University, Waltham, MA, USA.

Motivated by recent experiments, we study a system of self-propelled colloids that experience short-range attractive interactions and are confined to a surface. Using simulations we find that the phase behavior for such a system is reentrant as a function of activity: phase-separated states exist in both the low- and high-activity regimes, with a homogeneous active fluid in between. To understand the physical origins of reentrance, we develop a kinetic model for the system's steady-state dynamics whose solution captures the main features of the phase behavior. We also describe the varied kinetics of phase separation, which range from the familiar nucleation and growth of clusters to the complex coarsening of active particle gels.

I. INTRODUCTION

Active fluids composed of self-propelled units occur in nature on many scales, ranging from cytoskeletal filaments and bacterial suspensions to macroscopic entities such as insects, fish, and birds [1]. These systems exhibit strange and exciting phenomena such as dynamical self regulation [2], clustering [3–8], anomalous density fluctuations [9], and unusual rheological and phase behavior [10–13]. To elucidate the the microscopic origins of collective behavior, recent experiments have focused on developing simplified, controllable active fluids in nonliving systems, using chemically propelled particles undergoing self-diffusophoresis [14–17], Janus particles undergoing thermophoresis [18, 19], and vibrated monolayers of granular particles [20–22].

Motivated by these experiments, we recently studied [7] a minimal active fluid model: a system of self-propelled smooth spheres confined to two dimensions and interacting solely by excluded-volume repulsion. We discovered that activity in this system induces a continuous phase transition to a state in which a high density solid coexists with a low density fluid, complete with a binodal coexistence curve and critical point. The aggregation of particles into dense clusters in the absence of any attractive interactions occurs as a result of self-trapping [4, 5, 7]. Separately, recent studies have examined several active colloidal systems which do possess attractive interparticle interactions [14, 23, 24]. The latter study demonstrates that activity *suppresses* phase separation, an effect which those authors postulate is generic.

In this paper we investigate these opposing effects in a system of self-propelled particles endowed with both attractive interactions and nonequilibrium self-propulsion. We find that the phase diagram of such a system is **reentrant** as a function of activity (Fig 1). This effect can be observed by traversing the phase diagram by increasing activity while holding the attraction strength fixed. At low activity the system is phase-separated due to attractive interparticle interactions, while increasing activity to moderate levels suppresses phase separation and

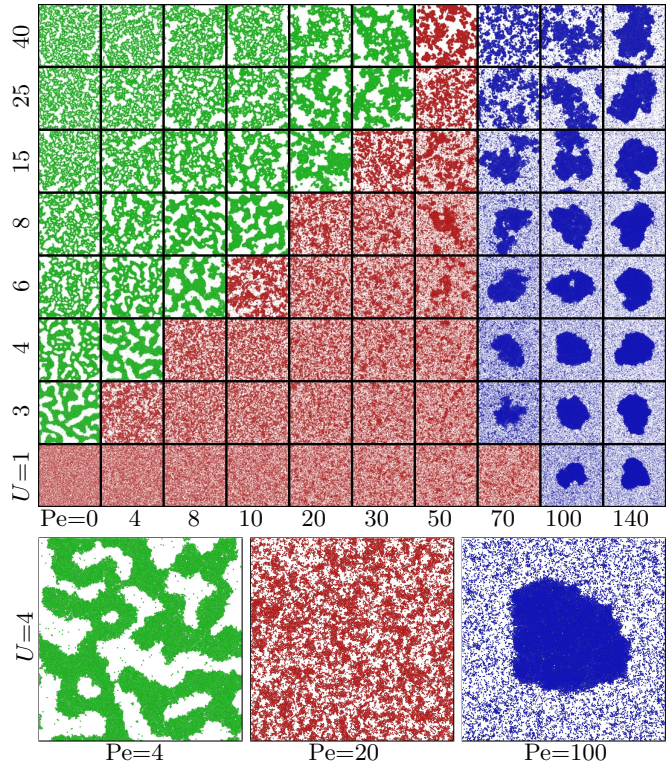


FIG. 1. **Top:** Phase diagram illustrated by simulation snapshots at time $t = 1000\tau$ with area fraction $\phi = 0.4$, as a function of interparticle attraction strength U and activity strength Pe . The colors are a guide to the eye distinguishing near-equilibrium gel states (green) from single-phase active fluids (red) and self-trapping-induced phase-separated states (blue). **Bottom:** Detail of reentrant phase behavior at $U = 4$ as Pe is increased. At $Pe = 4$ (left), the system is nearly thermal and forms a kinetically arrested attractive gel. Increasing Pe to 20 (center) suppresses phase separation and produces a homogeneous fluid characterized by transient density fluctuations. Increasing Pe further to 100 (right) results in athermal phase separation induced by self-trapping.

produces a homogeneous fluid. Increasing activity even further induces self-trapping which returns the system to a phase-separated state. We construct a simple kinetic model whose analytic solution captures the form of this unusual phase diagram and explains the mechanism by

* hagan@brandeis.edu

which activity can both suppress and promote phase separation in different regimes. We also describe the kinetics of phase separation, which differ significantly between the near-equilibrium and purely active phase-separated states. The behaviors we observe are robust to variations in parameter values, and thus could likely be observed in experimental systems of self-propelled, attractive colloids such as those studied in Refs. [14, 23, 24].

II. MODEL

Our model is motivated by recently developed experimental systems of self-propelled colloids sedimented at an interface [14, 23], and consists of smooth spheres immersed in a solvent and confined to a two-dimensional plane [7]. Each particle is active, exerting a constant propulsion force on the surrounding fluid. Since the particles are smooth spheres and we neglect hydrodynamic coupling, they do not interchange angular momentum and thus there are no systematic torques. However, the particles' self-propulsion directions undergo rotational diffusion; based on experimental observations [23], we confine the propulsion directions to be always parallel to the surface. For simplicity, interparticle interactions are modeled by the standard Lennard-Jones potential $V_{\text{LJ}} = 4\epsilon \left[\left(\frac{\sigma}{r} \right)^{12} - \left(\frac{\sigma}{r} \right)^6 \right]$ which provides hardcore repulsion as well as short-range attraction, with σ the nominal particle diameter, and ϵ the depth of the attractive well.

The state of the system is represented by the positions and self-propulsion directions $\{\mathbf{r}_i, \theta_i\}_{i=1}^N$ of the particles, and their evolution is governed by the coupled overdamped Langevin equations:

$$\dot{\mathbf{r}}_i = \frac{1}{\gamma} [\mathbf{F}_{\text{LJ}}(\{\mathbf{r}_i\}) + F_p \hat{\boldsymbol{\nu}}_i] + \sqrt{2D} \boldsymbol{\eta}_i^T \quad (1)$$

$$\dot{\theta}_i = \sqrt{2D_r} \eta_i^R \quad (2)$$

Here $\mathbf{F}_{\text{LJ}} = -\nabla V_{\text{LJ}}$, F_p is the magnitude of the self-propulsion force, and $\hat{\boldsymbol{\nu}}_i = (\cos \theta_i, \sin \theta_i)$. The Stokes drag coefficient γ is related to the diffusion constant by the Einstein relation $D = \frac{k_B T}{\gamma}$. D_r is the rotational diffusion constant, which for a sphere in the low-Reynolds-number regime is $D_r = \frac{3D}{\sigma^2}$. The η are Gaussian white noise variables with $\langle \eta_i(t) \rangle = 0$ and $\langle \eta_i(t) \eta_j(t') \rangle = \delta_{ij} \delta(t - t')$.

We non-dimensionalized the equations of motion using σ and $k_B T$ as basic units of length and energy, and $\tau = \frac{\sigma^2}{D}$ as the unit of time. Our Brownian dynamics simulations employed the stochastic Runge-Kutta method [25] with an adaptive time step, with maximum value $2 \times 10^{-5} \tau$. The potential V_{LJ} was cut off and shifted at $r = 2.5\sigma$.

III. PHASE BEHAVIOR

We parametrize the system by three dimensionless variables: the area fraction ϕ , the Péclet number $\text{Pe} = v_p \frac{\tau}{\sigma}$, and the strength of attraction $U = \frac{\epsilon}{k_B T}$. In order to limit our investigation to regions with nontrivial phase behavior, we fix the area fraction at $\phi = 0.4$. At this density, a passive system ($\text{Pe} = 0$) is supercritical for $U \lesssim 2.2$, and phase-separated for stronger interactions [26]. For purely repulsive self-propelled particles, the system undergoes athermal phase separation as a result of self-trapping for $\text{Pe} \gtrsim 85$, and remains a homogeneous fluid for smaller Pe [7].

To understand the phase behavior away from these limits, we performed simulations in a periodic box with side length $L = 200$ (with resulting particle count $N = 20371$) for a range of attraction strengths $U \in [1, 50]$ and propulsion strengths $\text{Pe} \in [0, 160]$. Except where noted, each simulation was run until time 1000τ . Systems were initialized with random particle positions and orientations except that (1) particles were not allowed to overlap and (2) each system initially contained a close-packed hexagonal cluster comprised of 1000 particles to overcome any nucleation barriers. To quantify clustering, we consider two particles bonded if their centers are closer than a threshold, and identify clusters as bonded sets of more than 200 particles. The cluster fraction f_c is then calculated as the total number of particles in clusters divided by N .

The behavior of the system is illustrated in Fig. 1 by representative snapshots, and in Fig. 3 with a contour plot of f_c . The most striking result is that the phase diagram is reentrant as a function of Pe . As shown in Fig. 1, low- Pe systems form kinetically arrested gels which gradually coarsen towards bulk phase separation. Increasing Pe to a moderate level destabilizes these aggregates and produces a homogeneous fluid, while increasing activity beyond a second threshold accesses a high- Pe regime in which self-trapping [4, 5, 7] restores the system to a phase-separated state.

As evident in Fig. 1, the widths of the low- Pe and high- Pe phase-separated regimes both increase with attraction strength U , eliminating reentrance for $U \gtrsim 40$. These trends can be schematically understood as follows. In the low-activity gel states, particles are reversibly bonded by energetic attraction. Particles thus arrested have random orientations, and so the mean effect of self-propulsion is to break bonds and pull aggregates apart. This opposes the influence of attraction, and so the width of the low- Pe gel region increases with U . By contrast, at high Pe we find that self-trapping is the primary driver of aggregation. As shown in the next section, energetic attractions act cooperatively with self-trapping in this regime to enable phase separation at lower Pe than would be possible with activity alone.

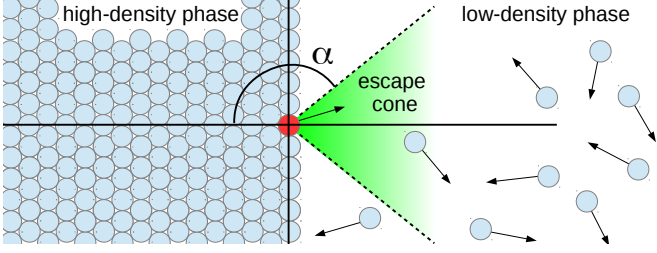


FIG. 2. Schematic representation of our kinetic model. The high- and low-density phases fill the left and right half-spaces. A particle on the cluster surface (red) escapes only if its direction points within the “escape cone” (green) defined by $F_p(\hat{\nu} \cdot \hat{n}) > F_{\max}$, while particles in the gas land on the surface at a rate proportional to the gas density and propulsion speed.

IV. KINETIC MODEL

To better understand the physical mechanisms underlying the reentrant phase behavior, we develop a minimal kinetic model to describe the phase separated state. By analytically solving the model we obtain a form for f_c which captures the major features of the phase behavior observed in our simulations. In the model we consider a single large close-packed cluster coexisting with a dilute gas which is assumed to be homogeneous and isotropic (Fig. 2). Particles in the cluster interior are assumed to be held stationary in cages formed by their neighbors, but their propulsion directions θ_i continue to evolve diffusively.

The rate per unit length at which gas-phase particles with a given orientation θ impinge on the flat surface of our model cluster is $\frac{1}{2\pi}\rho_g v_p \cos \theta$, with ρ_g the number density of the gas. Integrating over angles for particles traveling toward the cluster yields $k_{\text{in}} = \frac{\rho_g v_p}{\pi}$, the rate at which gas particles condense onto the cluster.

Next we estimate the rate of evaporation. We note that a particle on the cluster surface remains bound so long as the component of its propulsion force along the outward normal, $F_p(\hat{\nu} \cdot \hat{n})$, is less than F_{\max} , the maximum restoring force exerted by the binding potential. As shown in Fig. 2, this implies an “escape cone” in which the particle’s director must point in order for it to escape. The critical angle is $\alpha = \pi - \cos^{-1}\left(\frac{U f_{\max}}{\text{Pe}}\right)$, with f_{\max} the non-dimensionalized maximum restoring force scaled by the depth of the attractive well, which subsumes all relevant details of the binding force: $f_{\max} = \frac{F_{\max}}{U} \frac{\sigma}{k_B T}$.

We now consider the angular probability distribution of particles on the cluster surface $P(\theta, t)$. If we take as our initial condition the steady-state distribution $P(\theta, 0) = P(\theta)$, then the rate per unit length at which particles leave the cluster is $k_{\text{out}} = \frac{1}{\sigma} \frac{\partial}{\partial t} \int_{-\alpha}^{\alpha} P(\theta, t) d\theta \Big|_{t=0}$. The time evolution of P is governed by diffusion, with absorbing boundaries at the edges of the cone: $\frac{\partial P(\theta, t)}{\partial t} = D_r \frac{\partial^2 P(\theta, t)}{\partial \theta^2}$ and

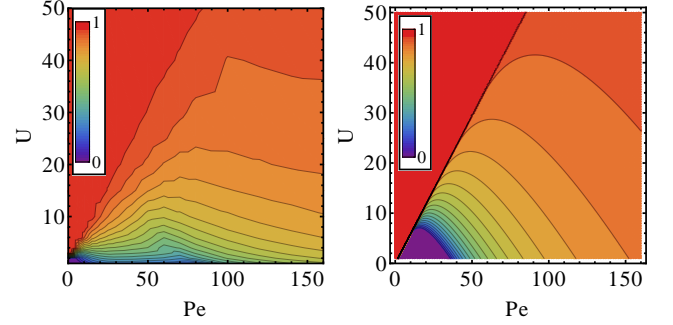


FIG. 3. **Left:** Fraction of particles in clusters f_c measured from simulations as a function of Pe and U . **Right:** f_c as predicted by our analytic theory (Eq. 3) which reproduces the major features of the phase diagram, including the gel region for $\text{Pe} < U$, the self-trapping region for high Pe, and the low- f_c fluid regime in between. The values of the fitting parameters are $\kappa = 2$ and $f_{\max} = 1.7$.

$P(\pm\alpha, t) = 0$, with general solution $P(\theta, t) = \sum_{q=1}^{\infty} A_q \cos\left(\frac{q\pi\theta}{2\alpha}\right) e^{-D_r \frac{q^2 \pi^2}{4\alpha^2} t}$. To simplify the analysis we note that higher-order terms decay rapidly in time, so the long-time behavior is dominated by the $q = 1$ term. We therefore discard higher-order terms and approximate the initial distribution as $P(\theta) = \frac{1}{2} \cos \theta$ (from the distribution of incident particles) and solve to find $k_{\text{out}} = \frac{D_r \pi^2}{4\sigma \alpha^2}$.

We further note from visual observation of our simulations that the departure of a surface particle opens a hole through which subsurface particles may escape if their propulsion directions point outward. [7]. We designate κ the total number of particles lost per surface particle that evaporates, and determine this value by fitting to our simulation data. The final expression for the evaporation rate is then $k_{\text{out}} = \frac{D_r \pi^2 \kappa}{4\sigma \alpha^2}$.

Equating k_{in} and k_{out} yields a steady-state condition which can, by assuming a close-packed cluster, be rewritten in terms of f_c :

$$f_c = \frac{16\phi\alpha^2\text{Pe} - 3\pi^4\kappa}{16\phi\alpha^2\text{Pe} - 6\sqrt{3}\pi^3\phi\kappa} \quad (3)$$

As shown in Fig. 3, this model reproduces the essential features of our system, including active suppression of phase separation at low Pe, activity-induced phase separation at high Pe, and a reentrant phase diagram. The model thus extends the analysis in Ref. [7] to describe the coupled effects of activity and energetic attraction. As noted in that reference, our model description of self-trapping can be considered a limiting case of the theory of Tailleur and Cates [4, 5] in which a self-propulsion velocity that decreases with density leads to an instability of the homogeneous initial state.

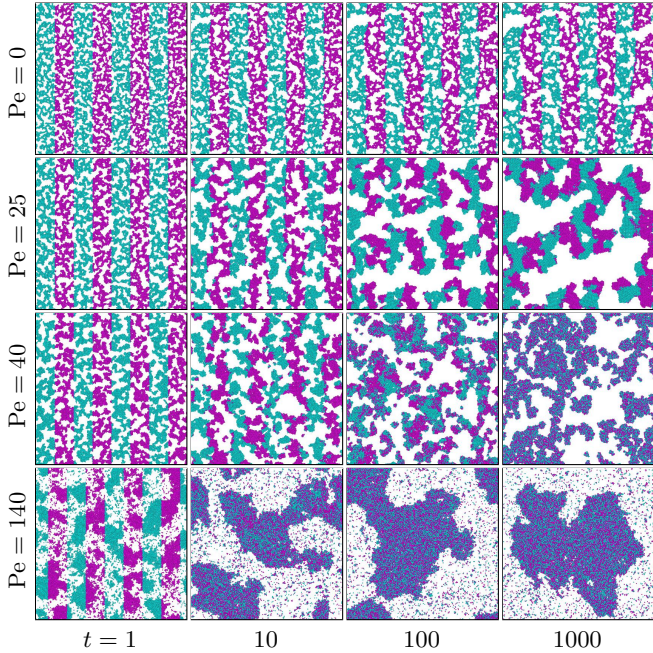


FIG. 4. Visual guide to phase-separation kinetics at fixed $U = 30$. To make mixing visible, particles are labeled in two colors based on their positions at $t = 1$. A passive system (top row) forms a space-spanning gel which gradually coarsens. The addition of activity (second row) greatly increases the rate at which the gel evolves. In both cases particles remain ‘local’ and largely retain the same set of neighbors. When Pe exceeds U (third row), activity is strong enough to break the gel filaments and a fluid of large mobile clusters results. While the instantaneous configurations appear structurally similar to the gels above, these systems quickly become well-mixed due to splitting and merging of clusters (see also Fig. 5). In the high- Pe limit (bottom row), self-trapping drives the emergence of a single well-mixed cluster surrounded by a dilute gas.

V. PHASE SEPARATION KINETICS

The kinetics of phase separation differ significantly between the low- Pe gel and high- Pe self-trapping regions. In low- Pe systems, thermal influences dominate and the kinetics are those of a colloidal particle gel [27]. Since the area fraction in our simulations is high, the gels we observe appear nonfractal. Thermal agitation gradually reorganizes the gel into increasingly dense structures [28, 29], leading toward a single compact cluster in the infinite-time limit. The presence of activity greatly accelerates the rate at which the gel evolves, as shown in Figs. 4 and 5.

As Pe is increased beyond the threshold value $Pe \approx U$, activity begins to overwhelm energetic attraction and the gel is ripped apart. This arrests the compaction, resulting in a plateau in the system’s total potential energy (Fig. 5). Just above this transition, the system resembles a fluid of large mobile clusters which rapidly split, translate, and merge (Fig. 4). This phase is clearly iden-

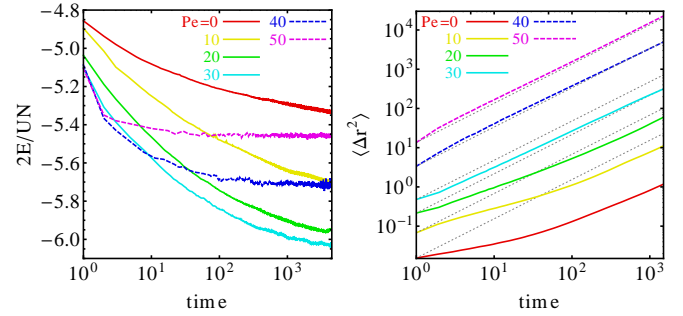


FIG. 5. Quantitative measurements of states with $U = 30$. **Left:** Mean interaction energy per particle (E represents the total system potential energy). Low- Pe gels are strongly arrested and do not approach bulk phase-separation on our simulation timescales; however, higher- Pe systems evolve much faster and nearly reach the bulk limit. When $Pe > U$ (dashed lines), coarsening is arrested as the gel breaks into a fluid of mobile clusters with a Pe -dependent characteristic size, leading to a plateau in the system energy. **Right:** Discrimination of gel from fluid states by mean-square displacement. Dotted gray lines have slope 1 and highlight the distinction between subdiffusive gels ($Pe < U$), and superdiffusive active fluids.

tified by mean-square displacement measurements (Fig. 5) which are superdiffusive for this active fluid, unlike the subdiffusive behavior found in gels. As Pe is further increased, the characteristic mobile cluster size decreases until the appearance of an ordinary single-phase active fluid is recovered.

Additional increase of Pe will eventually cross a second threshold into a phase-separated regime whose behavior is dominated by self-trapping. As reported previously [7], these systems undergo nucleation, growth, and coarsening stages in a manner familiar from the kinetics of quenched fluid systems, albeit with the unfamiliar control parameter Pe instead of temperature.

These three regimes are characterized by dramatically different particle dynamics. To illustrate these behaviors and their effect on particle reorganization timescales, in Fig. 4 we present snapshots from simulations in which initial particle positions are identified by color. We see that when attraction is dominant ($U > Pe$), each particle’s set of neighbors remains nearly static over the timescales simulated, indicative of long relaxation timescales due to kinetic arrest. In contrast, when activity dominates ($Pe > U$) particles rapidly exchange neighbors and the system becomes well-mixed. Importantly, note that particle dynamics cannot be directly inferred from the instantaneous spatial structures in the system. For example, while systems with low activity ($Pe < U$, Fig. 4 second row) and moderate activity ($Pe \gtrsim U$, Fig. 4 third row) appear structurally similar, the rate of particle mixing differs by orders of magnitude.

VI. CONCLUSIONS

Activity can both suppress and induce phase separation, and we have shown that these opposing effects can coexist in the same simple system. The resulting counterpoint produces a reentrant phase diagram in which two distinct types of phase separation exist, separated by a homogeneous fluid regime. This surprising result makes it possible to use two experimentally accessible control parameters (Pe and U) in concert to tune the phase behavior of active suspensions. This control is especially valuable because attractive interparticle interactions are common in experimental active systems, being

either intrinsic [14, 23] or imposed, such as by the addition of depletants [24]. An understanding of the complex phase behavior accessible to these systems is a critical stepping stone toward designing smart active materials whose phases and structural properties can dynamically respond to conditions around them.

VII. ACKNOWLEDGMENTS

This work was supported by NSF-MRSEC-0820492 (GSR, AB, MFH), as well as NSF-DMR-1149266 (AB). Computational support was provided by the Brandeis HPC.

[1] T. Vicsek and A. Zafeiris, *Physics Reports* **517**, 71 (2012).

[2] A. Gopinath, M. F. Hagan, M. C. Marchetti, and A. Baskaran, *Physical Review E* **85**, 061903 (2012).

[3] F. Peruani, A. Deutsch, and M. Bär, *Physical Review E* **74**, 1 (2006).

[4] J. Tailleur and M. Cates, *Phys. Rev. Lett.* **100**, 3 (2008).

[5] M. E. Cates and J. Tailleur, *EPL (Europhysics Letters)* **101**, 20010 (2013).

[6] S. R. McCandlish, A. Baskaran, and M. F. Hagan, *Soft Matter* **8**, 2527 (2012).

[7] G. S. Redner, M. F. Hagan, and A. Baskaran, *Physical Review Letters* **110**, 055701 (2013).

[8] Y. Fily and M. C. Marchetti, *Physical Review Letters* **108**, 235702 (2012).

[9] S. Ramaswamy, R. A. Simha, and J. Toner, *Europhysics Letters (EPL)* **62**, 196 (2003).

[10] L. Giomi, T. B. Liverpool, and M. C. Marchetti, *Physical Review E* **81**, 051908 (2010).

[11] D. Saintillan, *Physical Review E* **81**, 056307 (2010).

[12] M. Cates, S. Fielding, D. Marenduzzo, E. Orlandini, and J. Yeomans, *Physical Review Letters* **101**, 068102 (2008).

[13] T. Shen and P. G. Wolynes, *Proceedings of the National Academy of Sciences of the United States of America* **101**, 8547 (2004).

[14] J. Palacci, S. Sacanna, A. P. Steinberg, D. J. Pine, and P. M. Chaikin, *Science* **339**, 936 (2013).

[15] J. Palacci, C. Cottin-Bizonne, C. Ybert, and L. Bocquet, *Physical Review Letters* **105**, 1 (2010).

[16] W. F. Paxton, K. C. Kistler, C. C. Olmeda, A. Sen, S. K. St Angelo, Y. Cao, T. E. Mallouk, P. E. Lammert, and V. H. Crespi, *Journal of the American Chemical Society* **126**, 13424 (2004).

[17] Y. Hong, N. Blackman, N. Kopp, A. Sen, and D. Velegol, *Physical Review Letters* **99**, 1 (2007).

[18] H.-R. Jiang, N. Yoshinaga, and M. Sano, *Physical Review Letters* **105**, 1 (2010).

[19] G. Volpe, I. Buttinoni, D. Vogt, H.-J. Kümmerer, and C. Bechinger, *Soft Matter* **7**, 8810 (2011).

[20] V. Narayan, S. Ramaswamy, and N. Menon, *Science (New York, N.Y.)* **317**, 105 (2007).

[21] A. Kudrolli, G. Lumay, D. Volfson, and L. Tsimring, *Physical Review Letters* **100**, 2 (2008).

[22] J. Deseigne, O. Dauchot, and H. Chaté, *Physical Review Letters* **105**, 1 (2010).

[23] I. Theurkauff, C. Cottin-Bizonne, J. Palacci, C. Ybert, and L. Bocquet, *Physical Review Letters* **108**, 1 (2012).

[24] J. Schwarz-Linek, C. Valeriani, A. Cacciuto, M. E. Cates, D. Marenduzzo, A. N. Morozov, and W. C. K. Poon, *Proceedings of the National Academy of Sciences of the United States of America* **109**, 4052 (2012).

[25] A. Braňka and D. Heyes, *Phys. Rev. E* **60**, 2381 (1999).

[26] B. Smit and D. Frenkel, *The Journal of Chemical Physics* **94**, 5663 (1991).

[27] V. Trappe and P. Sandkühler, *Current Opinion in Colloid & Interface Science* **8**, 494 (2004).

[28] W. C. Poon, *Current Opinion in Colloid & Interface Science* **3**, 593 (1998).

[29] R. DArjuzon, W. Frith, and J. Melrose, *Physical Review E* **67**, 1 (2003).